A PARAMETRIC DESIGN OF COMPACT EXHAUST MANIFOLD JUNCTION IN HEAVY DUTY DIESEL ENGINE USING CFD

by

Hessamedin NAEIMI, Davood DOMIRY GANJI
Mofid GORJI, Ghasem JAVADIRAD, and Mojtaba KESHAVARZ

[a] Faculty of Mechanical Engineering, Babol University of Technology, Babol, Iran
[b] Iran heavy diesel MFG. Co. (DESA), Amol, Iran

Nowadays, computational fluid dynamics codes (CFD) are prevalently used to simulate the gas dynamics in many fluid piping systems such as steam and gas turbines, inlet and exhaust in internal combustion engines. In this paper, a CFD software is used to obtain the total energy losses in adiabatic compressible flow at compact exhaust manifold junction. A steady state one-dimensional adiabatic compressible flow with friction model has been applied to subtract the straight pipe friction losses from the total energy losses. The total pressure loss coefficient has been related to the extrapolated Mach number in the common branch and to the mass flow rate ratio between branches at different flow configurations, in both combining and dividing flows. The study indicate that the numerical results were generally in good agreement with those of experimental data from the literature and will be applied as a boundary condition in one-dimensional global simulation models of fluid systems in which these components are present.

key words: *total pressure loss coefficient, numerical simulation, compact exhaust manifold junction, experimental data*

Introduction

The appropriate selection of turbocharging system type and the reasonable design of exhaust manifold configurations in heavy-duty diesel engines is very significant since the performance of a four-stroke turbocharged diesel engine is greatly affected by the gas flow in the exhaust manifold [1–3]. At the present time, several different turbocharging systems are usually adopted: the constant pressure turbocharging system, the pulse turbocharging system, the pulse converter (PC) turbocharging system and the compact exhaust manifold or modular pulse converter (MPC) turbocharging system, etc. In the constant pressure turbocharging system, the exhaust ports of all cylinders are connected to a single manifold to damping unsteady gas flow from cylinders. Hence, the pressure in the turbine inlet is almost steady. This allows the turbine to operate at optimum efficiency at specified engine conditions. This matter is a major advantage of this type of turbocharging. However, the significant disadvantages of the constant pressure turbocharging are poor turbocharging acceleration and performance at low speed and load. In the case of the pulse turbocharging system, the exhaust gases coming from two or three cylinders, which have minimum interference in scavenging process base on the firing order, are discharged into a common branch exhaust pipe. It aims to make

[*] Corresponding author: E-mail: hessam.naeimi@gmail.com

maximum use of the energy available in the high pressure and temperature exhaust gases. This turbocharging system has good turbocharger acceleration and performance at low speed and part load. However, its application is limited by the number of the exhaust manifold and the design of the exhaust manifold with large numbers of cylinders is complex. In addition the turbine efficiency with one or two cylinder per turbine entry or at very high rating is poor [4]. Pulse converter turbocharging system has been developed to overcome the disadvantage of the pulse turbocharger. In this system, many cylinders are connected to a single low volume manifold. So that the pressure variation at the turbine entry is reduced and its result the turbine efficiency is improved. However, the PC turbocharging system has poor performance at very low speed/load and is only suitable for engines with certain numbers of cylinders (e.g. four, eight, sixteen and, etc.) [5]. Nowadays, the MPC turbocharging system has become popular because the structure of its exhaust manifolds is simple. In this kind of turbocharging system, as it is shown in fig.1, all the exhaust ports are connected to a common exhaust duct by a distinct pulse converter. This system intends to preserve the pulsing energy of exhaust gases coming from cylinders and transmit it to the turbine inlet while reduces the backflow toward cylinders during scavenging as possible [6].

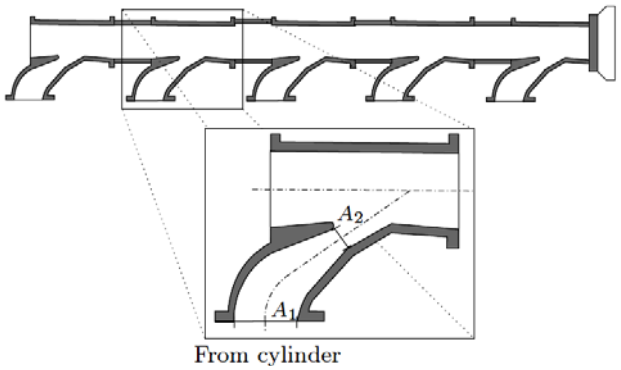

Figure 1. Modular pulse converter junction of Chan [17]

Nowadays, the one-dimensional models are used in the global simulation of steady and transient compressible flow in pipe systems, such as BOOST (AVL) [7], GT POWER [8]. These models are utilized as well as to analysis of internal combustion engine performance at various operating conditions. However, the fluid flow through the compact exhaust manifold junctions, as its geometry, is three-dimensional and highly turbulent. Since the total pressure loss coefficients must be obtained separately and added to these models as special boundary. Unfortunately there is not enough pressure loss data in literature especially for compressible flow in compact exhaust manifold. The largest source of the experimental result for pressure loss in 'T' junction have been perform by Miller[9]. Basset et al. [10] compared different modelling techniques. A multi-dimensional computer program was developed by Chiatti and Chiavola [11]. These cods were used to simulate the flow within different components of the exhaust system in internal combustion engine (ICE). Commercial codes, such as Star-CD, Fluent or Fire-AVL were used by Shaw et al. [12], and Gan and Riffat [13]. Abou-Haidar and Dixon [14] and Pearson et al. [15] utilized 1D and 2D models to simulate the wave propagation phenomenon. Most of the works have been focused on designing manifolds of ICE. In the present work, a commercial CFD package, FLUENT [16] is used to obtain the total energy losses in

adiabatic compressible flow at compact exhaust manifold junction. The numerical results were generally in good agreement with the steady flow measurements of Chan [17].

Mathematical model

The fluid flow studied is governed by three-dimensional compressible adiabatic steady-state form of the Reynolds-averaged Navier–Stokes (RANS) conservation equations and the additional equations describing the transport of other scalar properties. They may be written in Cartesian tensor notation as:

$$\frac{\partial}{\partial x_i}\left(\rho u_i\right)=0 \tag{1}$$

$$\frac{\partial}{\partial x_i}\left(\rho u_i u_j\right)=-\frac{\partial p}{\partial x_i}+\frac{\partial}{\partial x_j}\left[\mu\left(\frac{\partial u_i}{\partial x_j}+\frac{\partial u_j}{\partial x_i}\right)-\frac{2}{3}\mu\delta_{ij}\frac{\partial u_k}{\partial x_k}\right]$$
$$+\frac{\partial}{\partial x_j}\left(-\rho\overline{u_i' u_j'}\right)=-\frac{\partial p}{\partial x_i}+\frac{\partial}{\partial x_j}\bar{\bar{\tau}}_{eff} \tag{2}$$

$$\frac{\partial}{\partial x_i}\left(u_i h_0\right)=\frac{\partial}{\partial x_j}\left(u_i\bar{\bar{\tau}}_{eff}\right)=u_i\frac{\partial}{\partial x_j}\bar{\bar{\tau}}_{eff}+\Phi_\upsilon \tag{3}$$

Different turbulence models based on RANS equations is available for studying the Reynolds stresses and the turbulent diffusivity terms. In this work, the two equations turbulent model $k-\varepsilon$ RNG will be used and different turbulent models were compared. The RNG model has an additional term in its equation that significantly improves the accuracy for rapidly strained flows. The effect of swirl on turbulence is included in the RNG model, enhancing accuracy for swirling flows. The turbulence kinetic energy, k , and its rate of dissipation, ε , are obtained from the following transport equations:

$$\frac{\partial(\rho k)}{\partial t}+div\left(\rho k\vec{U}\right)=div\left[\frac{\mu_t}{\sigma_k}grad\ k\right]+2\mu_t E_{ij}.E_{ij}-\rho\varepsilon \tag{4}$$

$$\frac{\partial(\rho\varepsilon)}{\partial t}+div\left(\rho\varepsilon\vec{U}\right)=div\left[\frac{\mu_t}{\sigma_\varepsilon}grad\ \varepsilon\right]+C_{1\varepsilon}\frac{\varepsilon}{k}2\mu_t E_{ij}.E_{ij}-C_{2\varepsilon}\rho\frac{\varepsilon^2}{k} \tag{5}$$

$$\mu_t=\rho C_\mu\frac{k^2}{\varepsilon}\qquad C_\mu=0.0845 \tag{6}$$

The coefficients of eq. (4) and eq. (5) are shown in tab. 1.

Table 1. Coefficients of $k-\varepsilon\ RNG$ model

$C_{1\varepsilon}$	$C_{2\varepsilon}$	σ_k	σ_ε
1.42	1.68	1.0	1.3

Definition of junction pressure loss coefficient

The studying here for calculation of the pressure loss at compact exhaust manifold will be limited by duct configuration and flow direction. Actually, there are six individual flow types for a

generalized three-pipe junction (fig. 2) and twelve loss coefficients associated with it. In this study (as shown in fig. 2), we have considered two flow types, one from combining flow type and another dividing flow.

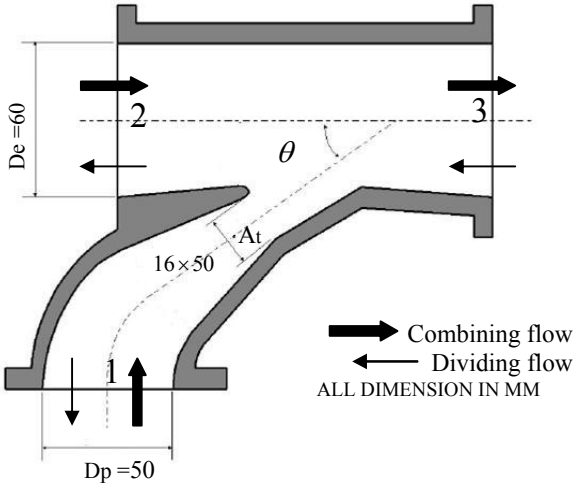

Figure 2. Schematic of modular pulse converter junction

The total pressure loss coefficient K_{ij}, given by Equation. (7), is defined as the ratio of the total pressure drop in the direction of positive mass flow to the dynamic-pressure (P_d) in the common branch that witch the total flow is passing [9].

$$K_{ij} = \frac{\Delta P_{ij}}{P_d} = \frac{\left(\frac{1}{2}\rho u_i^2 + P_{si}\right) - \left(\frac{1}{2}\rho u_j^2 + P_{si}\right)}{\frac{1}{2}\rho u_t^2} \tag{7}$$

where

$$u_t = \begin{cases} u_i & if\ Q_i > Q_j \\ u_j & if\ Q_i < Q_j \end{cases} \tag{8}$$

Notice that the dynamic-pressure (P_d) in the leg carrying the total flow for compressible flow is obtained from the following equation:

$$P_d = P_{0t}^* - P_{st}^* \tag{9}$$

So, the four loss coefficients for the combining and dividing flow as shown in fig. 2 are calculated as follows:

Combining flow:

$$K_{13} = \frac{\Delta P_{13}}{P_3} = \frac{\left(\frac{1}{2}\rho u_1^2 + P_{s1}\right) - \left(\frac{1}{2}\rho u_3^2 + P_{s3}\right)}{P_{03}^* - P_3^*} \tag{10}$$

$$K_{23} = \frac{\Delta P_{23}}{P_3} = \frac{\left(\frac{1}{2}\rho u_2^2 + P_{s2}\right) - \left(\frac{1}{2}\rho u_3^2 + P_{s3}\right)}{P_{03}^* - P_3^*} \tag{11}$$

Dividing flow:

$$K_{31} = \frac{\Delta P_{31}}{P_3} = \frac{\left(\frac{1}{2}\rho u_3^2 + P_{s3}\right) - \left(\frac{1}{2}\rho u_1^2 + P_{s1}\right)}{P_{03}^* - P_3^*} \tag{12}$$

$$K_{32} = \frac{\Delta P_{32}}{P_3} = \frac{\left(\frac{1}{2}\rho u_3^2 + P_{s3}\right) - \left(\frac{1}{2}\rho u_2^2 + P_{s2}\right)}{P_{03}^* - P_3^*} \tag{13}$$

When the Mach number of air flow is less than 0.2, the air passing of compact exhaust manifold can be considered incompressible. The loss coefficient for incompressible flow is independent of common branch much number and just changes with mass flow ratio. However, the value of loss coefficient for compressible flow does vary with common branch much number, too.

Computational domain

The flow domain as shown in fig.3 has a three-pipe intersection. An unstructured, non-uniform mesh, a detail of the grid in the intersection of the branches region, the mesh structure on the symmetry plane and a detail of the mesh at the cross-section are illustrated. Due to the symmetry of modular exhaust junction, in all flow configurations the computational domain can be considered one half of the actual volume. In order to make sure that the accuracy of results was independent of computation's grid, calculations were carried out with several different grid resolutions as well as modifying the distance of the wall-adjacent cells to the wall. For all mass flow rates simulated, the y^+ value is maintained within the recommended range, $30 < y^+ < 500$. The number of cells of the mesh finally used was 186,354.

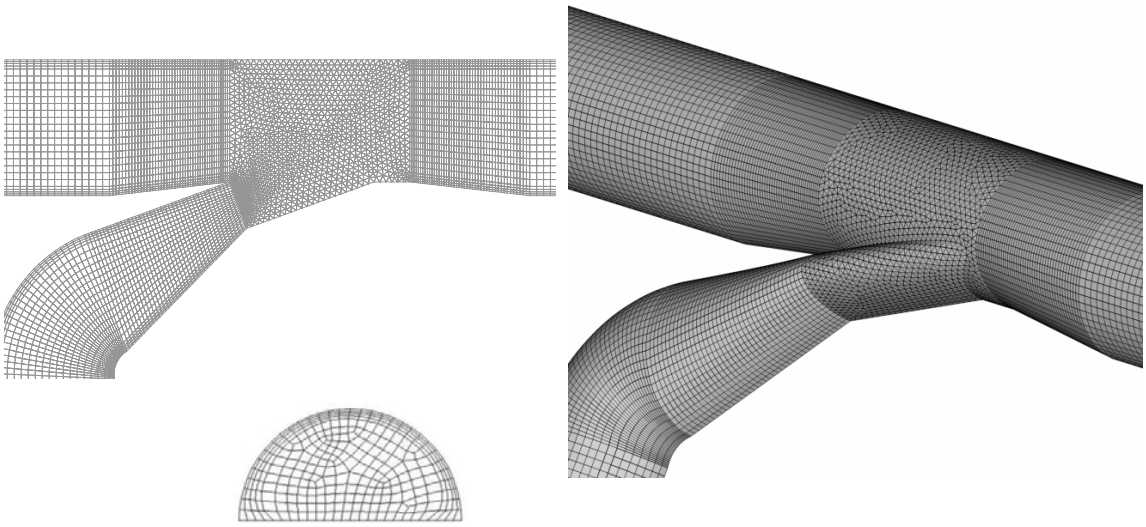

Figure3. 3D computational domain, mesh structure in the plane of symmetry and in the cross-sectional of a branch at compact manifold junction simulated

In all of the studied cases here, the much number of the outlet exhaust manifold is assumed constant and is 0.25. Outlet pressure and temperature was fixed 300 Pa and 300 K, respectively. So, based on the target mass flow rate ratio (q), desired mass flow rate for each branch has been studied. Since the air flow was supposed compressible, a mass flow rate and static pressure at the inlet and outlet boundary condition has been chosen, respectively. Also, for simulating the turbulent flow, the turbulence intensity and the hydraulic diameter were set to 3.5% and 50mm respectively as turbulence parameters in both of the combining and dividing flow. Flow is adiabatic and non-slip condition with wall roughness height is used for wall condition.

Evaluating the pipe wall friction factor

In estimating pressure loss due to compact exhaust manifold, the pressure measurements location is great importance. The pressure should be measured in fully developed flow region. So that the one dimensional Fanno flow model could be used. In other words, if the pressure measuring location was not selected correctly the result would not be reliable. Figure 4 demonstrates the total pressure changes in symmetry surface of different compact exhaust manifolds having different branch lengths.

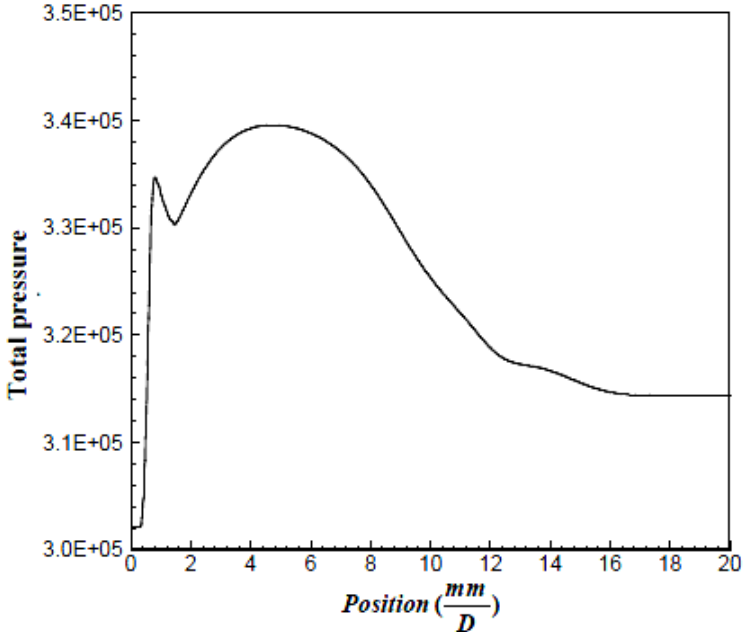

Figure 4. Total pressure curve in symmetry surface of common branch

As can be seen from this figure, total pressure of the flow in manifolds having length equal or greater then 18D remains constant. Thus, the flow condition for compact exhaust manifold having aforesaid branch length will be fully developed. The pipe friction factor is defined in Equation (14) as:

$$f = \frac{\tau_w}{\frac{1}{2}\rho u^2} \tag{14}$$

It is common practice, in wave-action simulation, to use a constant value of f in the region of 0.004 – 0.01. In fact the curve on the Moody diagram for a smooth pipe ($\Delta \approx 2.5\mu m$) gives value in

the range of 0.0035 to 0.008 for Reynolds numbers in the range of 1×10^4 to 5×10^5. For Reynolds numbers in the range $5\times10^3 \le \mathrm{Re} \le 10^8$ and relative roughness values in the range $10^{-6} \le (\Delta/D) \le 10^{-2}$, Swamee and Jain propose [18] the following relationship:

$$f = \frac{0.25}{\left[\log_{10}\left(\frac{\Delta}{3.7D} + \frac{5.74}{\mathrm{Re}}\right)\right]^2} \tag{15}$$

Equation (15) can be applied to give either a value for at every mesh point and time step of the calculation or to give an average value for each point section comprising manifold [19].

Using one-dimensional and adiabatic flow conditions between two points in Fanno flow, Mach number can be calculated from eq. (16). Then all thermo-fluid properties extrapolated can be obtained and the total pressure loss coefficient computed from eq. (7).

$$f\frac{(x_2 - x_1)}{D} = \frac{\gamma+1}{2\gamma}\ln\left[\frac{1+\left[(\gamma-1)/2\right]M_2^2}{1+\left[(\gamma-1)/2\right]M_1^2}\right] - \frac{1}{\gamma}\left(\frac{1}{M_2^2} - \frac{1}{M_1^2}\right) - \frac{\gamma+1}{2\gamma}\ln\frac{M_2^2}{M_1^2} \tag{16}$$

Results and discussion

Different turbulent models implemented in fluent have been compared. The $k-\varepsilon$ standard and RNG with standard wall functions, $k-w$ standard and Spalart-Allmaras turbulence models have been used in preliminary simulations at different flow configurations.

In fig. 5, the total pressure loss coefficients obtained with each turbulence model are represented against a mass flow rate between branches and compare with experimental data by Chan [17].

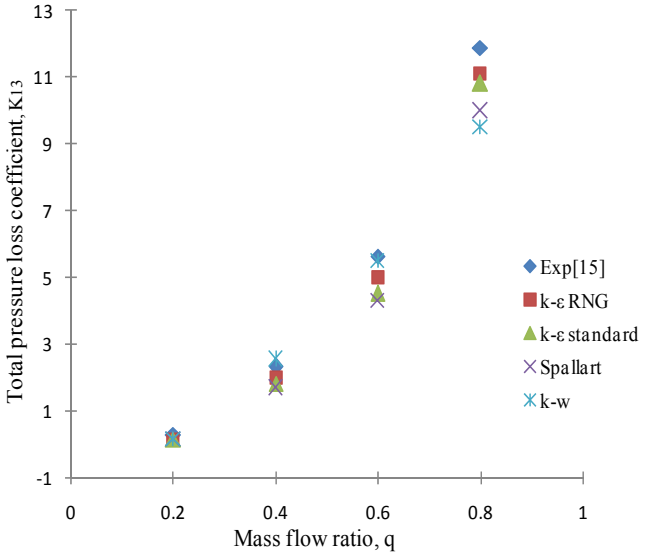

Figure 5. Comparison between different turbulence models (Combining flow)

It can be observed that in the both flow types, loss coefficient predicted by $k-\varepsilon$ RNG turbulence model is in a good agreement with reference data. As a result, this turbulence model will be used in all simulations.

Combining flow

The compact exhaust manifold with combining flow type has been simulated with different mass flow rate ratio, q= 0.1 to 0.9, for combining flow type. Figure 6 shows the simulation results on the velocity contour on the symmetry plane in the compact manifold near the junction for three flow ratios.

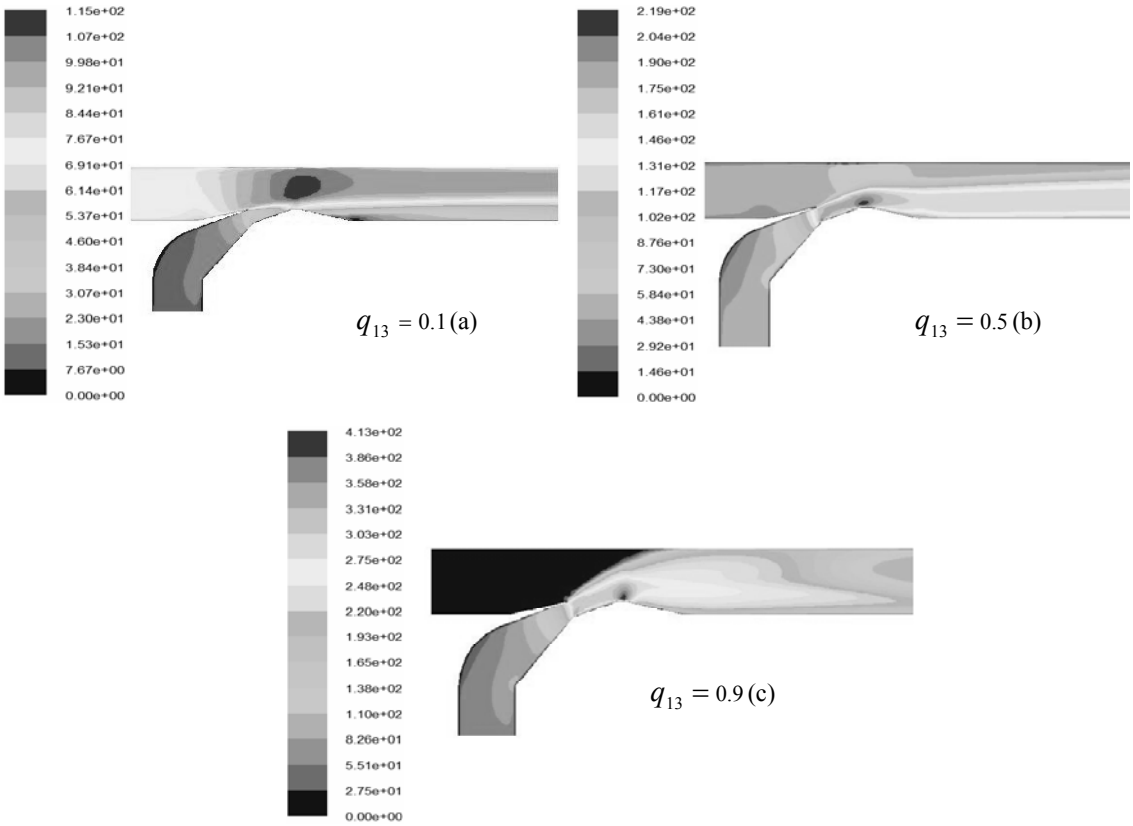

Figure 6. Predicted combining flows for the centre plane of the compact manifold

Mainly, the multi-dimensional undesirable phenomena, such as flow separation, turbulent mixing, eddies production and etc. caused to decrease the total energy of fluid flow. By increasing the mass flow rate in branch 1, the flow velocity increases in throat area and then the effect of flow separation and vortex formation due to the changing cross section in flow upstream increases. So, the pressure loss coefficient is increased. Most published experimental data for pressure loss coefficients are for T-junctions with a straight branch. The only data for compact exhaust manifold comparable with the present investigation is that reported by Chan [17]. A comparison between the predicted and reported pressure loss coefficients is given in tab. 2. The predicted pressure loss coefficient is in good agreement with the reported value.

Table 2. Comparison of junction pressure loss coefficients for combining flow

q	K_{13}		K_{23}	
	Predicted	Exp.[17]	Predicted	Exp.[17]
0.1	−0.7	N/A	−3.44	N/A
0.2	0.21	0.29	−2.16	−1.97
0.3	1.2	N/A	−1.7	N/A
0.4	2.01	2.31	−1.11	−1.28
0.5	3.19	N/A	−0.74	N/A
0.6	5.2	5.64	−0.35	−0.23
0.7	7.46	N/A	0.05	N/A
0.8	10.4	11.88	0.32	0.48
0.9	13.57	N/A	0.52	N/A

Throat area (At) is one of the important parameters in compact manifold design. Compact exhaust manifold works as fluid diode which allows exhaust gas to move from cylinder to the turbine and limits the flow returning from manifold to the cylinder. This will be done by decreasing the throat area. With this decrement in throat area, the velocity will be increased and the pressure will be decreased. So, it will avoid back pressure in exhaust manifold hence flow returning to the cylinder will be limited. Hence, in this study the effect of the area ratio of At/Ap on the pressure loss coefficient has been investigated. Figures 6 and 7 show the variation of the loss coefficients K_{13} and K_{23} with mass flow rate for three different At/Ap of 0.3, 0.35 and 0.4. As shown in figures 6 and 7, the pressure loss coefficient in each branch will be increased with flow rate. In lower flow rates, the ratio of At/Ap has not significant effect on the pressure loss coefficient. However, in the higher flow ratio of the branch 1 to branch 3, K_{13} will be increased with At/Ap decrease. The situation happens in reverse form for K_{23}. It can be concluded from above that in a specific flow rate, magnitude of K_{23} and K_{13} will be decreased with At/Ap ratio increase.

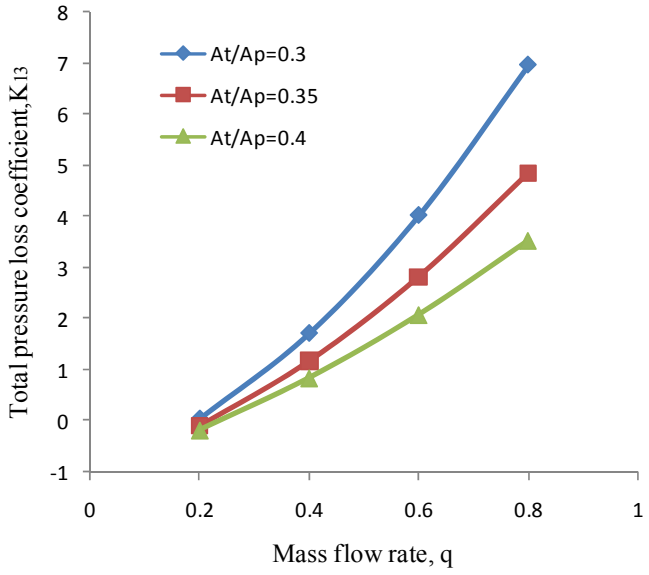

Figure 7. Effect of At/Ap on pressure loss coefficient K_{13}

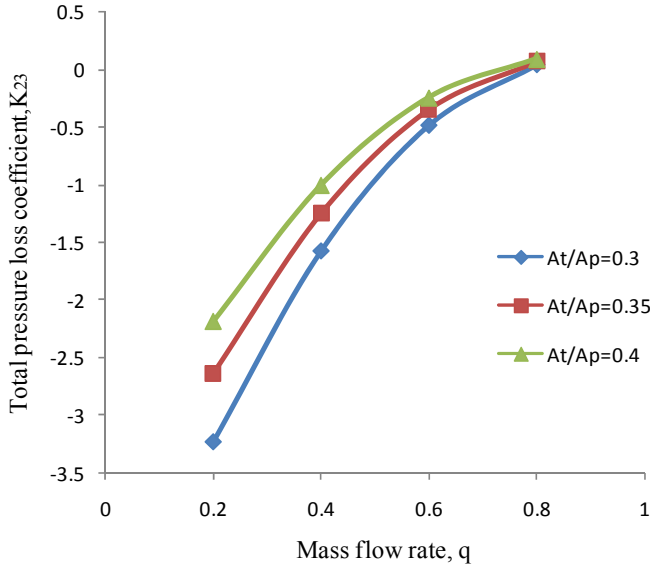

Figure 8. Effect of At/Ap on pressure loss coefficient K_{23}

Dividing flow

Figure 9 shows the predicted dividing flow-patterns near the intersection for three different flow ratios. In low mass flow rate ratio (q=0.1) eddies are seen in side branch (branch "1"). By addition of flow ratio (q=0.5), the location of recirculation region in the branch changes and velocity increases in throat. By further increases of velocity, we accost chock (Fig. 9c). The hoped-for full range up to q = 0.9 could not be obtained despite adequate pressure being available upstream. In dividing flow, q ranged from 0.1 up to a maximum of about 0.6, which was effectively the choking limit. The predicted and reported pressure loss coefficients for dividing flows for flow ratios up to 0.6 is shown in tab. 3.

Table 3. Comparison of junction pressure loss coefficients for combining flow

q	K_{31}		K_{32}	
	Predicted	Exp.[17]	Predicted	Exp.[17]
0.1	0.46	N/A	0.386	N/A
0.2	1.11	1.53	0.29	0.316
0.3	1.8	N/A	0.28	N/A
0.4	3.5	3.92	0.3	0.285
0.5	6.0	N/A	0.32	N/A
0.6	10.6	9.57	0.35	0.309

As seen from the table, the simulation results are in good agreement with experimental data. For mass flow rate ratio more than 0.6, a shock wave is developed when the supersonic flow passes through the side branch "1". So, the pressure loss coefficient can't be obtained for larger mass flow rate.

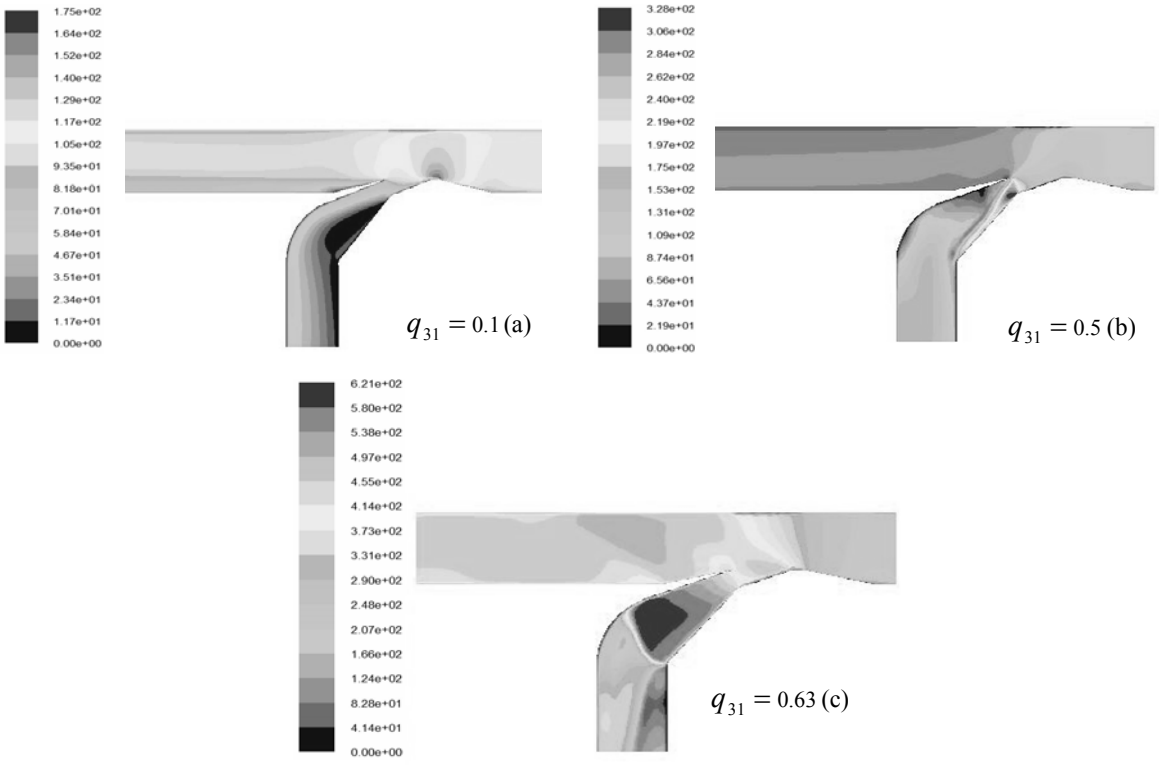

Figure 9. Predicted dividing flows for the centre plane of the compact manifold

Conclusion

In this paper a computational fluid flow model, k-ε RNG, has been used to obtain the pressure loss coefficient in compact exhaust manifold junction. Also, to subtract the frictional losses from the total energy losses, the one-dimensional Fanno flow model has been used. A comparison between the predicted and experimental data shows this model and methodology is in generally good for the estimate of the pressure losses in both combining and dividing flow. But the maximum mass flow rate of the divided flow was 0.6, because a limit caused by chocking.

Finally, these coefficients can be used as boundary conditioning in one-dimensional software such as GT-Power to simulate the complete engine cycle. As a suggestion for future work, we can optimize the design parameters of the compact manifold.

Nomenclature

A	– Pipe cross-sectional area,[m^2]	μ	– Absolute viscosity,[Pas]
D	– Internal diameter,[m]	μ_t	– Turbulent viscosity,[Pas]
E_{ij}	– Rate of deformation,[s^{-1}]	ρ	– Gas density,[kgm^{-3}]
f	– Friction factor,[-]	μ	– Absolute viscosity,[Pas]
h_0	– Stagnation enthalpy,[Jkg^{-1}]	τ_{eff}	– Apparent stress tensor,[Pa]
k	– Turbulent kinetic energy,[m^2s^{-1}]	Φ_v	– Rayleigh dissipation function,[Pas^{-1}]
K	– Total pressure loss coefficient,[-]	δ_{ij}	– Kronecher delta,[-]
M	– Total pressure loss coefficient,[-]	θ	– Junction lateral branch angle

M^* – Extrapolated Mach number up to Junction,[-]
P_0 – Stagnation pressure,[Pa]
P_s – Static pressure,[Pa]
Q – Mass flow rate,[kgs^{-1}]
q – Mass flow rate ratio,[-]
Re – Reynolds number,[-]
u_i – Time-averaged gas velocity,[ms^{-1}]
U – Average gas velocity,[ms^{-1}]
y^+ – Sublayer scaled distance
– $y^+ = \rho u_\tau y / \mu$,[-]
Re – Reynolds number,[-]
u_i – Time-averaged gas velocity,[ms^{-1}]

Greek letters

γ – Ratio of specific heats $\gamma = c_p / c_v$,[-]
Δ – Non-dimensional roughness,[m]
ε – Turbulent dissipation rate,[m^2s^{-3}]

Subscripts

1,2 – Inlet (combining flow) or outlet (dividing flow) branches
3 – Common branch
* – Extrapolated properties to the junction
i,j – Branch leg index
3 – Common branch
–
–
–
–
–
–
–
–
–

References

[1] Kesgin, U., Effect of turbocharging system on the performance of a natural gas engine, *Energy Conversion and Management,*Vol. 46, 2005, PP.11–32.

[2] Galindo, J., Lujan, J.M., Serrano, J.R., Dolz, V., Guilain, S., Design of an exhaust manifold to improve transient performance of a high-speed turbocharged diesel engine, *Experimental Thermal and Fluid Science*, Vol. 28, 2004, PP. 863–875.

[3] Kesgin, U., Study on the design of inlet and exhaust system of a stationary internal combustion engine, *Energy Conversion and Management,*Vol. 46, 2005, PP. 2258–2287.

[4] Hu, X., Lawless, PB., Predictions of on-engine efficiency for the radial turbine of a pulse turbocharged engine. *SAE paper* 2001-01-1238, 2001.

[5] Bassett, M.D., Pearson, R.J., Winterbone, D.E., Steady-flow loss-coefficient estimation for exhaust manifold pulse converter type junctions. *SAE Paper* 1999-01-0213, 1999.

[6] Yang, S.Y., Deng, K.Y., Cui, Y., Simulation and experimental research on a mixed pulse converter turbocharging system, *Journal of Automobile Engineering*, Vol. 221, 2007, PP. 215–223.

[7] BOOST, User Manual for AVL BOOST, AVL List GmbH, Department for Applied Thermodynamics, 1996, <http://www.avl.com>.

[8] GT Power – User's manual. GT Suite Version 5.1. Gamma Technologies Inc., USA, 2000.

[9] Miller DS. Internal flow systems. 2nd ed. Cran®eld: *The British Hydromechanics Research Association*, 1990.

[10] Basset, M.D., Winterbone, D.E., Pearson, R.J., Modelling engines with pulse converted exhaust manifolds using one-dimensional techniques, 2000, *SAE paper* 2000-01-0290.

[11] Chiatti, G., Chiavola, O., Multicode prediction of the influence of the exhaust system on the performance of a turbocharged engine, *J. Eng. Gas Turbines Power*, ASME 124 (3) (2002) 695–701.

[12] Shaw, C.T., Lee, D.J., Richardson, S.H., Pierson, S., Modelling the effect of plenum–runner interface geometry on the flow through an inlet system, 2000, *Paper SAE* 2000-01-0569.

[13] Gan, G., Riffat, S.B., Numerical determination of energy losses at duct junctions, *Appl. Energy* 67 (2000) 331–340.
[14] Abou-Haidar, N.I., Dixon, S.L., Pressure losses in combining subsonic flows through branched ducts, Trans. ASME, J.Turbomach. 114 (1) (1992) 264–270.
[15] Pearson, R.J., Masset, M.D., Batten, P., Winterbone, D.E., Multidimensional wave propagation in pipe junctions, 1999, *Paper SAE* 1999-01-1186.
[16] FLUENT user's guide. USA: Fluent Inc., 1995.
[17] Chan, C.L., An investigation of the performance of a diesel engine fitted with compact manifold, M.Sc. Thesis, *University of Manchester Institute of Science and Technology*, 1985.
[18] Swamee, P. K., Jain, A. K., Explicit equations for pipe-flow problems, *J. Hydraulic Div. Proc. ASCE*, May 1976, PP. 657-664.
[19] Winterbone, D.E., Pearson, R.J., Theory of Engine Manifold Design. Wave Action Methods for IC Engines, Professional Engineering Publishing, London, 2000.

Authors′ address:

Hessamedin NAEIMI (corresponding author)
Faculty of Mechanical Engineering,
Babol University of Technology,
Babol, Iran
hessam.naeimi@gmail.com

Davood DOMIRY GANJI
Faculty of Mechanical Engineering,
Babol University of Technology,
Babol, Iran

Mofid GORJI

Faculty of Mechanical Engineering,
Babol University of Technology,
Babol, Iran

Ghasem JAVADIRAD
Iran heavy diesel MFG. Co. (DESA),
Amol, Iran

Mojtaba KESHAVARZ
Iran heavy diesel MFG. Co. (DESA),
Amol, Iran